Surface Characterization of Quaternized Polysulfone Films and Biocompatibility Studies

Silvia Ioan, Raluca Marinica Albu, Ecaterina Avram, Iuliana Stoica, Emil Ghiocel Ioanid

Petru Poni Institute of Macromolecular Chemistry, Iasi 700487, Romania

Received 2 November 2009; accepted 11 September 2010
DOI 10.1002/app.33380
Published online 16 February 2011 in Wiley Online Library (wileyonlinelibrary.com).

ABSTRACT: A novel quaternized polysulfone with *N*-dimethyloctylammonium groups was investigated with respect to its surface properties, hydrophobicity, interactions with blood, and morphology. The history of the films formed from *N*,*N*-dimethylformamide/methanol and *N*,*N*-dimethylformamide/water solutions and the compositions of the solvent/nonsolvent mixtures influenced the surface morphology. Thus, atomic force microscopy investigations of the films showed pores and nodules of different sizes and intensities, which depended on the content of methanol or water in the solvent mixtures. Hydrophilicity modification, evidenced by the apolar components and the electron-acceptor and electron-donor parameters of the polar components of the surface tension parameters, was correlated with atomic force microscopy data. Surface wettability trends were analyzed on the basis of the free energy of hydration between the prepared films and water and the work of adhesion. The adhesion of red blood cells to the modified polysulfone showed the influence of the hydrophobic properties. © 2011 Wiley Periodicals, Inc. J Appl Polym Sci 121: 127–137, 2011

Key words: atomic force microscopy (AFM); biocompatibility; polyelectrolytes; surfaces

INTRODUCTION

In recent years, considerable attention has been devoted to the investigation of new applications of polysulfones (PSFs), mainly because of their specific properties. PSFs and their derivatives are widely used as new functional materials in biochemical, industrial, and medical fields because of their structural and physical properties, such as their good optical properties, high thermal and chemical stability, mechanical strength, resistance to extreme pH values, and low creep.[1–5] They are noncrystalline polymers; their chain rigidity is derived from the relatively inflexible and immobile phenyl and SO_2 groups, whereas their toughness is derived from the connecting ether oxygen.[6] The application of PSF is focused on blood-contact devices (e.g., hemodialysis, hemodiafiltration, and hemofiltration in the form of membranes),[7–10] cell- and tissue-contact devices (e.g., bioreactors made of hollow-fiber membranes),[11–13] and nerve generation (through semipermeable, hollow PSF membranes).[14–16] Although these materials have excellent overall properties, their intrinsically hydrophobic nature restricts their use in membrane applications requiring hydrophilicity, such as saline-solution perfusion, artificial kidney membranes, and cell culture bioreactors. Hydrophobic surfaces possess high interfacial free energies in aqueous solutions, and this unfavorably influences their blood and cell compatibility during the initial contact stage.

On the other hand, chloromethylated and quaternized PSFs have several interesting properties that recommend them for a wide range of industrial and environmental applications. Their functional groups can modify hydrophilicity (which is especially interesting for biomedical applications),[17] antimicrobial activity,[18] and solubility characteristics[19,20] and thus allow higher water permeability and better separation.[21,22] In addition, functional groups are an intrinsic requirement for affinity, ion-exchange, and other specialty membranes.[23]

In previous publications, the synthesis[24–26] and some solution properties[19,20,27–31] of modified PSFs have been presented. Studies of the quaternization reaction of chloromethylated polysulfones (CMPSFs) have been carried out to obtain water-soluble polymers with various amounts of ionic chlorine. The conformational behavior in solution and the experimental and theoretical results for the preferential adsorption coefficients versus the solvent composition have been discussed in correlation with the interaction parameters of quaternized PSFs and mixed solvents.[20,28,31] Surface wettability and hydrophilicity trends as well as the morphological characteristics of some modified PSFs have also been analyzed for biomaterials and for semipermeable membrane applications.[30,32]

Correspondence to: S. Ioan (ioan_silvia@yahoo.com).

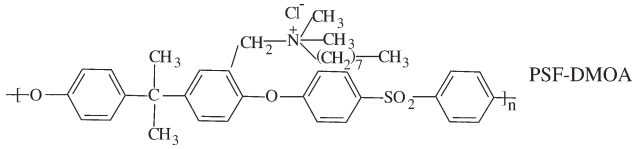

Scheme 1 General structure of PSF–DMOA.

The objective of this study was to investigate the morphological characteristics of quaternized PSFs obtained from CMPSFs with a tertiary amine [*N*-dimethyloctylamine (DMOA)]. The corresponding films, obtained from solutions of *N,N*-dimethylformamide (DMF)/methanol (MeOH) and DMF/water mixtures, were analyzed by atomic force microscopy (AFM) to determine the influence of the casting solutions on the morphological properties. The results were correlated with the hydrophilic/hydrophobic properties of the polymers and the blood compatibility.

EXPERIMENTAL

Materials

UDEL-3500 PSF (number-average molecular weight = 39,000, weight-average molecular weight/number-average molecular weight = 1.625), a commercial product from Union Carbide Corporation, Texas City, USA, was purified by repeated reprecipitation from chloroform and dried for 24 h *in vacuo* at 40°C before it was used in the synthesis of CMPSF. A mixture of commercial paraformaldehyde with an equimolar amount of chlorotrimethylsilane as a chloromethylation agent and stannic tetrachloride as a catalyst was used for the chloromethylation reaction of PSF at 50°C. The reaction time necessary to obtain CMPSF was 72 h.[24] Finally, the samples were dried *in vacuo* at 40°C.

Polysulfone with *N*-dimethyloctylammonium chloride groups (PSF–DMOA) was synthesized through the reaction of CMPSF (6.58% chlorine) with a tertiary amine (DMOA). The quaternization reaction was performed in DMF with a CMPSF/tertiary amine molar ratio of 1:1.5 for 24 h. The quaternary polymers were isolated from the reaction medium by precipitation in diethyl ether, washed with diethyl ether, and dried for 48 h *in vacuo* at room temperature. The ionic chlorine and total chlorine contents were determined by potentiometric titration (TTT1C titrator, Radiometer, Copenhagen, Denmark) with aqueous solutions of 0.02*N* $AgNO_3$. The ratios of the ionic chlorine and total chlorine contents showed that the quaternization reaction of CMPSF occurred at a transformation degree close to 98%. Thus, almost all chloromethylene groups could be considered quaternized. The ionic chlorine content, total ionic chlorine content, and molecular weight of the structural units of PSFs with quaternary groups were 3.23%, 3.29%, and 627.30, respectively. Also, the number-average molecular weight, which was determined from the polymerization degree of PSF (90) and the molecular weight of the structural units of PSF–DMOA, was 55,800.

The general chemical structure of the modified PSF under study is presented in Scheme 1.

Contact-angle measurements

Quaternized PSF (PSF–DMOA) was dissolved in DMF and DMF/MeOH (in the composition range of 75/25 to 45/55% v/v) to reach a concentration of 10 g/dL and in DMF/water (in the composition range of 75/25 to 50/50% v/v) to reach a concentration of 4 g/dL. The solutions were cast onto a glass plate and were initially solidified by slow drying in a saturated atmosphere with the solvent and finally solidified by drying at 50°C *in vacuo*. The PSF–DMOA films thus prepared were subjected to surface analysis as well as AFM investigations both before and after the plasma treatment.

Uniform drops of test liquids (2 μL) were deposited onto the film surface, and the contact angles were measured after 30 s with a video-based, optical contact-angle measuring device equipped with a Hamilton syringe in a temperature-controlled environmental chamber (home-made apparatus). All measurements were performed in air at 25°C. Repeated measurements of a given contact angle were all within ±3°. As probe liquids, double-distilled water, formamide, ethylene glycol (EG), methylene iodide (CH_2I_2), and 1-brom-naphthalene (1-Bn) were used as purchased at the maximum obtainable purity.

Low-pressure plasma treatment

The low-pressure plasma treatment consisted of exposing the PSF–DMOA films to a low-temperature and low-pressure glow discharge. Cold air plasma was produced with a high-frequency system (frequency = 1.3 MHz, intensity = 3000 V/cm, pressure = 0.58 mbar, power = 100 W) equipped with inner aluminum electrodes (home-made apparatus). The duration of the plasma treatment was 15 min; the contact-angle measurements were taken immediately after its application.

AFM

AFM images were obtained on an SPM Solver Pro-M instrument (NT-MDT; Moscow, Russia). An NSG10/Au silicon tip (NT-MDT Moscow, Russia) with a 10-nm curvature radius and a 255-kHz oscillation mean frequency was used to investigate the membrane surface morphology. The apparatus was operated in a semicontact mode over different scan areas; scan areas of 20 × 20 μm^2 and 60 × 60 μm^2 were selected for analyzing the influence of the casting solutions

TABLE I
Surface Tension Parameters of the Liquids Used for Contact-Angle Measurements

Liquid	γ_{lv} (mN/m)	γ_{lv}^{d} (mN/m)	γ_{lv}^{p} (mN/m)	γ_{lv}^{+} (mN/m)	γ_{lv}^{-} (mN/m)
Water[33]	72.80	21.80	51.00	25.50	25.50
Formamide[34]	58.00	39.00	19.00	2.28	39.60
EG[35]	48.00	29.00	19.00	47.00	1.92
CH_2I_2[36]	50.80	50.80	0	0.72	0
1-Bn[37]	44.40	44.40	0	0	0
Red blood cells[38]	36.56	35.20	1.36	0.01	46.2

on the morphological properties of PSF–DMOA films both before and after the plasma treatment.

RESULTS AND DISCUSSION

Surface tension parameters

The methods used for the determination of the surface tension were based on contact-angle measurements between the liquid meniscus and the quaternized PSF surface. A contact angle below 90° indicated that the substrate was readily wetted by the test liquid, whereas an angle over 90° showed that the substrate resisted wetting. The surface tension parameters (at room temperature, i.e., 22–25°C)[33–38] of water, formamide, EG, CH_2I_2, and 1-Bn that were used in the calculations of the surface tension parameters of the PSF–DMOA films are presented in Table I.

For the calculation of the surface tension parameters, the geometric mean (GM) method [eqs. (1) and (2)][39–41] and the acid–base (LW/AB) method [eqs. (3)–(6)][42–44] were used; the contact angles between these solvents and the PSF–DMOA films before and after the plasma treatment are presented in Table II. A decrease in the contact angles after the plasma treatment indicated higher oxygenation of the surface leading to higher hydrophilicity:

$$\frac{1+\cos\theta}{2}\cdot\frac{\gamma_{lv}}{\sqrt{\gamma_{lv}^{d}}}=\sqrt{\gamma_{sv}^{p}}\cdot\sqrt{\frac{\gamma_{lv}^{p}}{\gamma_{lv}^{d}}}+\sqrt{\gamma_{sv}^{d}} \quad (1)$$

$$\gamma_{sv}=\gamma_{sv}^{d}+\gamma_{sv}^{p} \quad (2)$$

where θ is the contact angle determined for different test liquids (Table I) and γ is the surface tension. Subscripts *lv* and *sv* denote liquid vapor and surface vapor, respectively, and superscripts *p* and *d* denote the polar and disperse components:

$$1+\cos\theta=\frac{2}{\gamma_{lv}}\cdot\left(\sqrt{\gamma_{sv}^{LW}\cdot\gamma_{lv}^{LW}}+\sqrt{\gamma_{sv}^{+}\cdot\gamma_{lv}^{-}}+\sqrt{\gamma_{sv}^{-}\cdot\gamma_{lv}^{+}}\right) \quad (3)$$

$$\gamma_{sv}^{AB}=2\cdot\sqrt{\gamma_{sv}^{+}\cdot\gamma_{sv}^{-}} \quad (4)$$

$$\gamma_{sv}^{LW/AB}=\gamma_{sv}^{LW}+\gamma_{sv}^{AB} \quad (5)$$

where superscripts *LW* and *AB* indicate the disperse and polar components obtained from the γ_{sv}^{-} electron-donor interactions and the γ_{sv}^{+} electron-acceptor interactions, respectively, and superscript *LW/AB* indicates the total surface tension.

According to the GM method, the solid surface tension components γ_{sv}^{d} and γ_{sv}^{p} were determined from the slope and intercept of the linear

TABLE II
Contact Angles of Different Liquids on Untreated and Plasma-Treated Quaternized PSF Films Prepared from Solutions of DMF/MeOH and DMF/Water Solvent Mixtures

Mixed solvent (% v/v)		Contact angle (°)				
		Water	Formamide	EG	CH_2I_2	1-Bn
100/0 DMF/MeOH	Untreated	72	46	45	32	15
	Treated	19	7	9	27	13
75/25 DMF/MeOH	Untreated	78	62	50	32	16
	Treated	15	7	9	25	11
50/50 DMF/MeOH	Untreated	58	55	39	28	16
	Treated	26	18	10	30	15
45/55 DMF/MeOH	Untreated	77	62	43	35	20
	Treated	25	20	11	30	17
75/25 DMF/water	Untreated	66	49	43	34	21
	Treated	—	—	7	15	9
60/40 DMF/water	Untreated	65	43	37	36	25
	Treated	—	—	5	18	7
50/50 DMF/water	Untreated	70	46	36	31	14
	Treated	—	—	5	16	11

TABLE III
Surface Tension Parameters and Contributions of the Polar Component to the Total Surface Tension for Untreated and Plasma-Treated PSF and CMPSF Films (Prepared from Chloroform Solutions) and for Quaternized PSF Films (Prepared from Solutions of DMF/MeOH and DMF/Water Solvent Mixtures) According to the GM Method [Eqs. (1) and (2)]

	Untreated films				Plasma-treated films			
Polymer film/ casting solvent	γ_{sv}^{d} (mN/m)	γ_{sv}^{p} (mN/m)	γ_{sv} (mN/m)	$\gamma_{sv}^{p}/\gamma_{sv}$ (%)	γ_{sv}^{d} (mN/m)	γ_{sv}^{p} (mN/m)	γ_{sv} (mN/m)	$\gamma_{sv}^{p}/\gamma_{sv}$ (%)
PSF in chloroform	17.28	11.21	28.49	39.35	16.42	42.90	59.32	72.32
CMPSF in chloroform	14.84	14.80	29.64	49.94	14.48	47.82	62.30	76.76
PSF–DMOA in DMF/MeOH (% v/v)								
100/0	40.93	5.06	45.99	11.02	37.89	27.11	65.01	41.70
75/25	39.60	2.95	42.55	6.93	38.03	27.75	65.78	42.19
50/50	43.56	1.85	45.21	4.09	37.50	25.33	62.85	40.30
45/55	39.05	3.63	42.68	8.51	37.11	25.74	62.85	40.95
PSF–DMOA in DMF/water (% v/v)								
75/25	38.41	7.54	45.96	16.41	46.43	6.51	52.94	12.30
60/40	38.52	8.60	47.12	18.25	37.51	7.70	45.21	17.03
50/50	41.44	5.92	47.36	12.50	37.11	6.73	43.85	15.35

dependence with eq. (1);[45] the known surface tension components[33–37] of different liquids (Table I) and contact angles (Table II) were used.

As for eq. (3) (the LW/AB method), literature data indicate that three polar liquids and a set of three equations may be used if the values of the liquid parameters, such as γ_{sv}^{-} and γ_{sv}^{+}, are not too close.[46,47] Della Volpe et al.[48] showed that improper utilization of three liquids without dispersive liquids or with two prevalently basic or prevalently acidic liquids strongly increases ill conditioning of the system. The different estimates of the acid–base components obtainable for the same solid by different triplets of liquids do not necessarily imply that this method is inconsistent but may simply reflect the large inaccuracies affecting the results because of ill conditioning. Also, researchers have postulated that the contact angles should be measured with a liquid surface tension higher than the anticipated solid surface tension, that is, $\gamma_{lv} > \gamma_{sv}$.[49]

Equation (3), written for different liquids, led to equation systems for determining the surface tension components. Five solvents were used in our investigation, with CH_2I_2 and 1-Bn employed as apolar solvents. Tables III and IV show the results for the surface tension components evaluated with both methods. The electron-donor and electron-acceptor parameters obtained by the LW/AB method are also presented. The apolar and polar surface tension parameters were influenced by the solvent/nonsolvent compositions from which the films had been prepared. Some studies reported that the chain shape of a polymer in solution could affect the morphology of the polymer in bulk.[32,35,50–52] Thus,

TABLE IV
Surface Tension Parameters and Contributions of the Polar Component to the Total Surface Tension for Untreated and Plasma-Treated Quaternized PSF Films Prepared from DMF/MeOH and DMF/Water Solutions According to the Acid–Base Method [Eqs. (4)–(6)]

Mixed solvent		γ_{sv}^{LW} (mN/m)	γ_{sv}^{+} (mN/m)	γ_{sv}^{-} (mN/m)	γ_{sv}^{AB} (mN/m)	$\gamma_{sv}^{LW/AB}$ (mN/m)
DMF/MeOH (% v/v)						
100/0	Untreated	42.41	0.38	1.43	1.48	43.88
	Plasma-treated	43.32	1.73	5.45	6.14	49.46
75/25	Untreated	42.69	0.19	0.83	0.79	43.49
	Plasma-treated	43.59	2.59	5.04	7.22	48.63
50/50	Untreated	43.11	1.54	1.97	1.77	44.88
	Plasma-treated	42.902	0.71	5.24	3.85	46.75
45/55	Untreated	41.29	1.04	0.46	1.39	42.68
	Plasma-treated	42.45	1.23	4.86	4.89	47.38
DMF/water (% v/v)						
75/25	Untreated	41.37	0.50	1.15	1.52	42.89
60/40	Untreated	40.22	0.79	3.52	3.33	43.55
50/50	Untreated	42.80	0.47	1.33	1.58	44.39

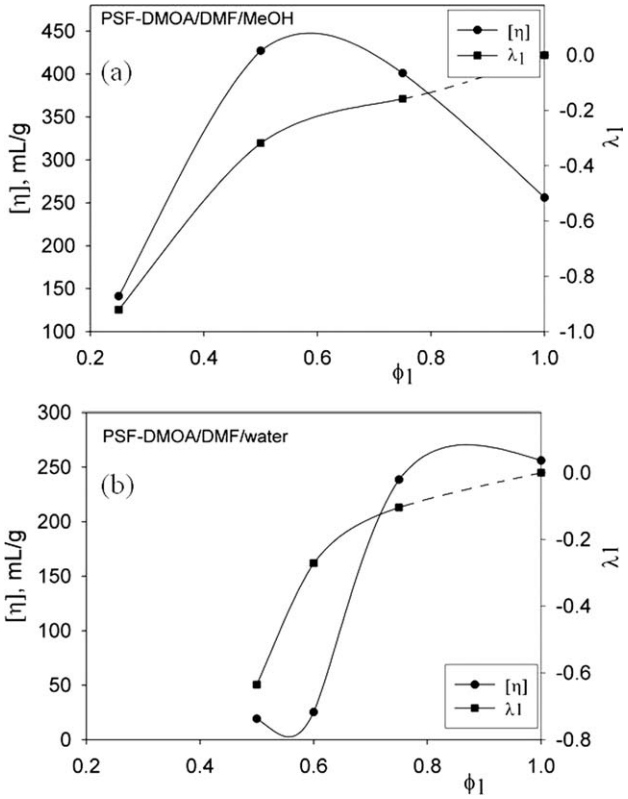

Figure 1 Influence of the DMF volume fraction (ϕ_1) on the intrinsic viscosity ([η]) and adsorption coefficient (λ_1) for PSF–DMOA in (a) DMF/MeOH and (b) DMF/water mixtures at 25°C.

Figure 1 plots the modification of the chain conformation of PSF–DMOA from variations in the intrinsic viscosity and adsorption coefficient with the DMF composition. According to previously obtained data, the PSF–DMOA coil dimensions possessed maximum values around DMF volume fractions of 0.60 and 0.75 in DMF/MeOH and DMF/water, respectively.[31]

At DMF volume fractions below 0.25 in DMF/MeOH and 0.5 in DMF/water, PSF–DMOA precipitated. Thus, the precipitation was caused by the nature of the alkyl radicals and by the nonsolvent content in the system. Therefore, for given compositions of the DMF/MeOH and DMF/water solvent mixtures, one of the components was preferentially adsorbed by the quaternized PSF molecules in the direction of the thermodynamically most effective mixture. These aspects influenced the surface properties of the polymer. Moreover, according to previously obtained data,[30] PSF showed the lowest hydrophilicity, which was induced by the aromatic rings connected by one carbon and two methyl groups, oxygen elements, and sulfonic groups, whereas chloromethylation of PSF with the functional group —CH_2Cl increased the hydrophilicity (see the surface tension values for PSF and CMPS in Table III). On the other hand, all PSF–DMOA films possessed low

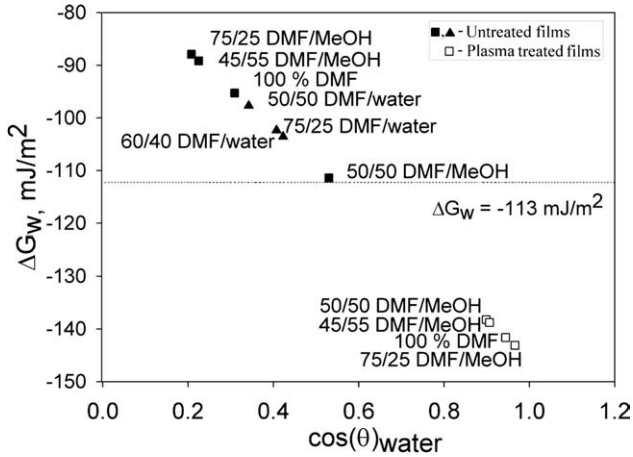

Figure 2 ΔG_w versus θ_{water} for PSF–DMOA.

polar surface tension parameters and reflected the influence of the mixed solvent composition. The hydrophobic character was imparted by the octyl radical from the *N*-dimethyloctylammonium chloride pendent group. In contrast to these results, a previous study showed that *N*-dimethyl(β-hydroxy)ethylammonium hydrophilic side groups caused strongly hydrophilic character in quaternized PSF.[30] Also, according to Tables III and IV, the polar terms from these data, γ_{sv}^{p} and γ_{sv}^{AB}, contributed less to the total surface tension parameters. Furthermore, the electron-donor interactions (γ_{sv}^{-}) exceeded the electron-acceptor interactions (γ_{sv}^{+}) according to a consideration of the electron-donor capacity of the octyl radical.

Low-pressure plasma treatment causes significant changes in the surface tension of a polymer. Generally, a plasma treatment applied to PSF membranes induces modifications of the surface properties because the highly energetic particles interact with the polymer surface. They may generate several kinds of reactions, the mechanisms of which are still unknown, such as breakage of the covalent bonds

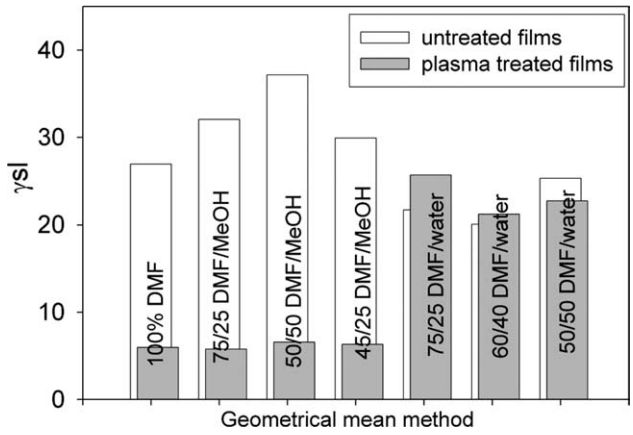

Figure 3 γ_{sl} for both untreated and plasma-treated PSF–DMOA films prepared in different DMF/MeOH and DMF/water solvent mixtures.

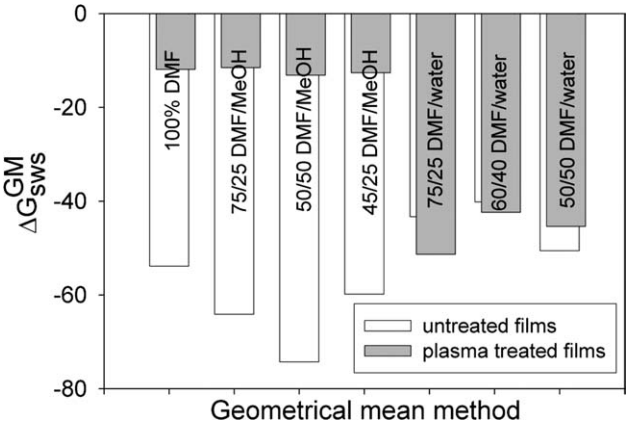

Figure 4 ΔG^{GM}_{sws} between two particles of PSF–DMOA in the water phase for both untreated and plasma-treated PSF–DMOA films prepared in different DMF/MeOH and DMF/water solvent mixtures.

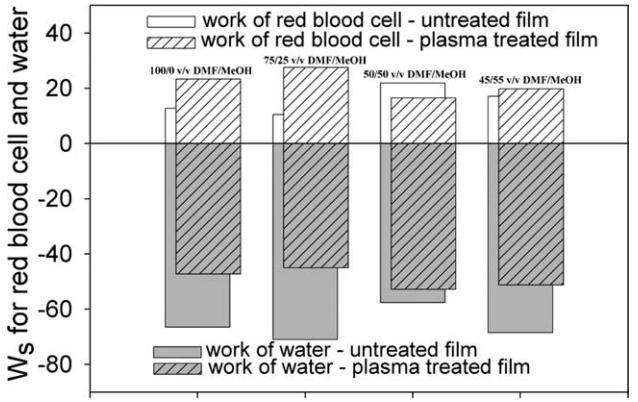

Figure 5 W_s for water and red blood cells over the surfaces of untreated and plasma-treated PSF–DMOA films prepared in different DMF/MeOH solvent mixtures.

along the chain, crosslinking, grafting, interactions of surface free radicals, alterations of existing functional groups, and incorporation of chemical groups originating in the plasma. However, polymer etching (involving a large set of destructive reactions removing the surface material and able to enlarge the pore diameter), modification of the surface chemistry (i.e., alteration of the surface chemistry through changes in the functionalities), and plasma polymer deposition (including processes allowing the deposition of materials on the surface as a thin layer) are the three main groups of processes that should be considered for analysis.[53,54]

Table III shows that the polar components of the surface tension significantly increased after the plasma treatment for the films prepared in DMF/MeOH solvent mixtures. This observation arises also from Table II: the relatively hydrophobic surface (i.e., a higher contact angle for water) was converted into a more hydrophilic one (a lower contact angle for water) by the plasma treatment for all studied samples. Also, Table III shows that the values of the $\gamma^{p}_{sv}/\gamma_{sv}$ ratio increased after the plasma treatment. Table II shows that the contact angles of the polar solvents (water and formamide) after the plasma treatment could not be measured because of their absorption into the polymer film structure. Thus, measurements of the contact angles were realized with only 1-Bn and CH_2I_2, which are apolar solvents, and EG, which has a low electron-donor character and is a polar solvent (Table I).

Surface free energy (ΔG_w) and interfacial free energy (ΔG^{GM}_{sws})

The effect of the history of the films formed from solutions on the surface properties was analyzed by the measurement of ΔG_w, which expresses the balance between surface hydrophobicity and hydrophilicity[55]:

$$\Delta G_w = -\gamma_{lv} \cdot (1 + \cos\theta_{water}) \quad (6)$$

where θ_{water} is the contact angle determined for water. γ_{lv} and θ_{water} are presented in Tables I and II, respectively.

The literature[44,55] specifies that with $\Delta G_w < -113$ mJ/m^2, a polymer can be considered more hydrophilic, whereas with $\Delta G_w > -113$ mJ/m^2, it should be considered more hydrophobic. These considerations led to the idea that ΔG_w evidenced high

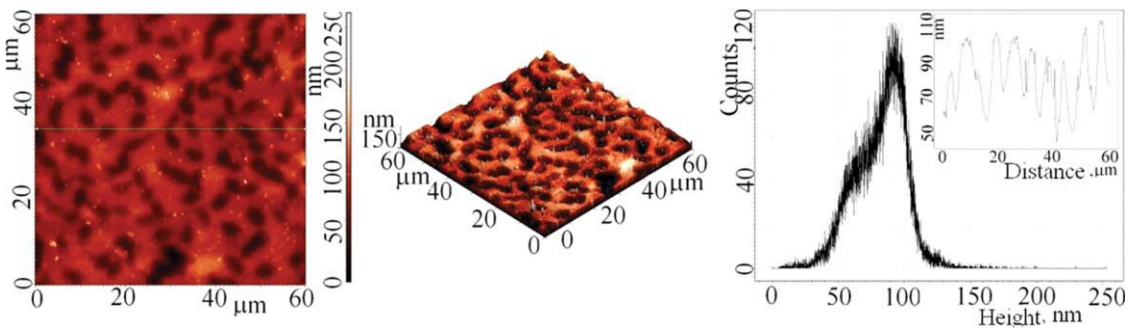

Figure 6 2D and 3D AFM images (scanned area = 60 × 60 μm^2) of PSF–DMOA films obtained from a DMF solution as well as the histogram and surface profile (small plot). [Color figure can be viewed in the online issue, which is available at wileyonlinelibrary.com.]

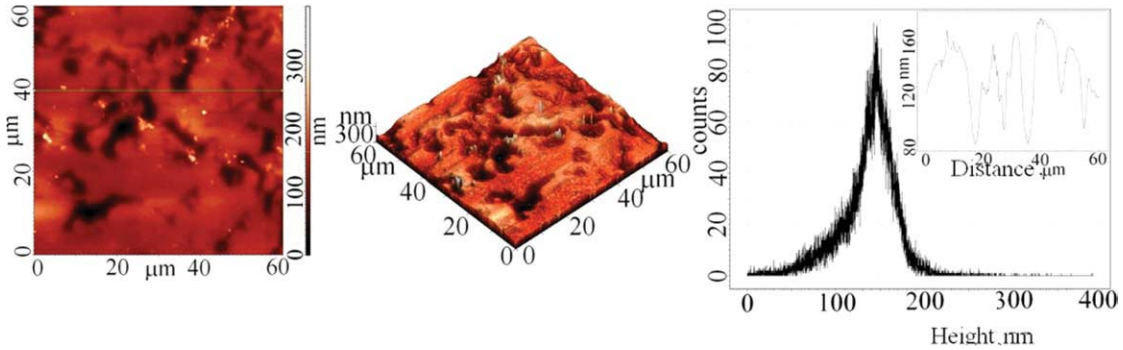

Figure 7 2D and 3D AFM images (scanned area = 60 × 60 μm^2) of PSF–DMOA films obtained from a 75/25 (v/v) DMF/MeOH solution as well as the histogram and surface profile (small plot). [Color figure can be viewed in the online issue, which is available at wileyonlinelibrary.com.]

hydrophobicity depending on the conditions of the film preparation, its value decreasing during plasma treatment (Fig. 2). The morphology of the films, induced by the history of their preparation from DMF/water solvent mixtures, was significantly changed by the plasma treatment, such that the water was completely adsorbed onto the surface. This made it impossible to measure the contact angles.

ΔG_{sws}^{GM} [eq. (7)] between two particles of PSF–DMOA in the water phase was evaluated on the basis of γ_{sl}, which denotes the solid–liquid interfacial tension in the GM method [eq. (8)]. γ_{sv}^{d} and γ_{sv}^{p} [eq. (8)] are presented in Table III:

$$\Delta G_{sws}^{GM} = -2 \cdot \gamma_{sl} \tag{7}$$

$$\gamma_{sl} = \left(\sqrt{\gamma_{lv}^{p}} - \sqrt{\gamma_{sv}^{p}}\right)^2 + \left(\sqrt{\gamma_{lv}^{d}} - \sqrt{\gamma_{sv}^{d}}\right)^2 \tag{8}$$

With the interfacial surface tension data presented in Figure 3, Figure 4 shows negative values for ΔG_{sws}^{GM} and indicates an attraction between the two polymer surfaces immersed in water; hence, these materials are considered hydrophobic.[56,57]

Also, the hydrophobicity of these polymers, described by the work of spreading over the surface (W_s) for water, represents the difference between the work of adhesion (W_a) and the work of cohesion (W_c) of water:

$$W_s = W_a - W_c = 2 \cdot [(\gamma_{sv}^{LW} \cdot \gamma_{lv}^{d})^{1/2} + (\gamma_{sv}^{+} \cdot \gamma_{lv}^{-})^{1/2} + (\gamma_{sv}^{-} \cdot \gamma_{lv}^{+})^{1/2}] - 2 \cdot \gamma_{lv} \tag{9}$$

According to the negative values of ΔG_{sws}^{GM} for modified PSFs, W_s for water (Fig. 5) had high negative values caused by surfaces with strong hydrophobicity; W_a for water was very low in comparison with W_c. The plasma treatment led to an increase in W_s because of the decrease in hydrophobicity that it caused.

Red blood cell compatibility

To analyze the possibility of using PSF–DMOA as a biomaterial and to establish its compatibility with blood, eq. (9), in which W_s describes the work of spreading of blood,[38] was used. When blood is exposed to a biomaterial surface, cell adhesion occurs, and the extent of adhesion determines the life of the implanted biomaterial because cellular adhesion to biomaterial surfaces can activate coagulation and immunological cascades. Therefore,

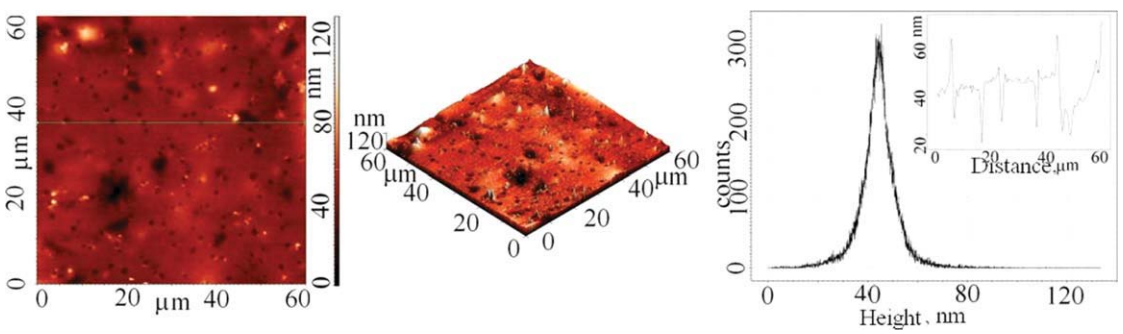

Figure 8 2D and 3D AFM images (scanned area = 60 × 60 μm^2) of PSF–DMOA films obtained from a 50/50 (v/v) DMF/MeOH solution as well as the histogram and surface profile (small plot). [Color figure can be viewed in the online issue, which is available at wileyonlinelibrary.com.]

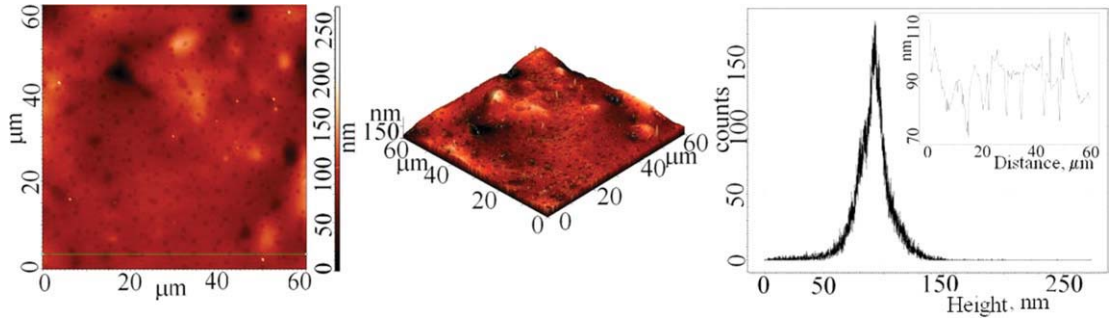

Figure 9 2D and 3D AFM images (scanned area = 60 × 60 μm^2) of PSF–DMOA films obtained from a 45/55 (v/v) DMF/MeOH solution as well as the histogram and surface profile (small plot). [Color figure can be viewed in the online issue, which is available at wileyonlinelibrary.com.]

cellular adhesion has a direct bearing on the thrombogenicity and immunogenicity of a biomaterial and thus dictates its blood compatibility. In this article, we suggest W_a for blood cells as a parameter for characterizing biomaterials versus cell adhesion. Thus, the materials exhibiting lower W_a values should lead to a lower extent of cell adhesion than those with higher W_a values. Considering the surface energy parameters for red blood cells (Table I), we estimated W_s for blood cells with eq. (9); we used the surface tension parameters for red blood cells (γ_{lv}, γ_{lv}^d, γ_{lv}^+, and γ_{lv}^-) in Table I and the surface free parameters for films prepared from DMF/MeOH solutions in Table IV. Figure 5 shows positive W_s values for cells and suggests higher W_a values in comparison with W_c and implicitly good compatibility between the modified PSF and the blood cells. Moreover, the good hydrophobicity could be correlated with the good adhesion of blood cells to the surfaces of the PSF films. These evaluations could be used to predict the cell adhesion and biocompatibility characteristics of materials. A low plasma treatment generally increased or decreased W_s for blood; this depended on the composition of the solvent mixtures in which the PSF–DMOA films were prepared.

Surface morphology

AFM was used to examine the film surfaces and measure their surface topography. Figures 6–9 plot two-dimensional (2D) and three-dimensional (3D) structures and also histograms and surface profiles (small plots) of PSF–DMOA films prepared with DMF/MeOH solvent mixtures of various compositions (100/0, 75/25, 50/50, and 45/25 v/v). According to these images, increasing the nonsolvent content in the casting solutions favored modification of the surface morphology. Thus, the average surface roughness decreased with increasing MeOH content and favored increases in the pore number and pore characteristics (area, depth, diameter, and mean width) according to Table V. The quality of the solvent mixtures over the studied domain increased with the addition of the nonsolvent according to Figure 1.

On the other hand, the presence of water as a nonsolvent in the solutions used for casting films

TABLE V
Pore Characteristics and Surface Roughness Parameters of Untreated Quaternized PSF Films Prepared from DMF/MeOH and DMF/Water Solutions with 20 × 20 μm^2 Scanned Areas Corresponding to 2D AFM Images

	Pore characteristics						Surface roughness		
Solvent mixture	Number of pores	Area (μm^2)	Depth (nm)	Diameter (μm)	Length (μm)	Mean width (μm)	Average roughness (nm)	Root mean square roughness (nm)	Nodule height from height profile (nm)
DMF/MeOH (% v/v)									
100/0	9	10.43	25.64	3.33	6.24	1.45	14.11	16.82	58
75/25	—	—	—	—	—	—	14.43	19.90	82
50/50	34	0.70	11.37	0.89	1.56	0.42	3.09	4.41	17
45/55	44	0.80	16.02	0.98	1.53	0.49	2.77	4.24	28
DMF/water (% v/v)									
75/25	5	3.12	13.65	1.97	3.26	0.96	1.59	2.34	15
60/40	27	0.04	19.54	0.22	0.35	0.11	9.19	11.83	70
50/50	18	2.09	5.55	1.46	2.63	0.64	1.52	2.17	8

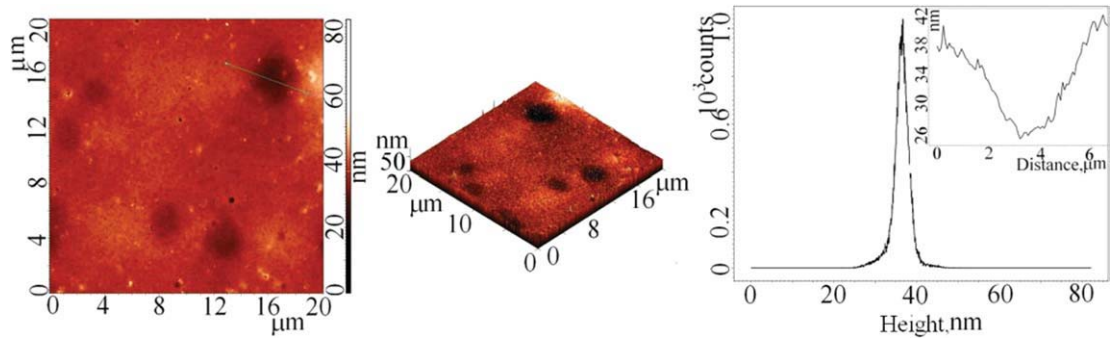

Figure 10 2D and 3D AFM images (scanned area = 20 × 20 μm^2) of PSF–DMOA films obtained from a 75/25 (v/v) DMF/water solution as well as the histogram and surface profile (small plot). [Color figure can be viewed in the online issue, which is available at wileyonlinelibrary.com.]

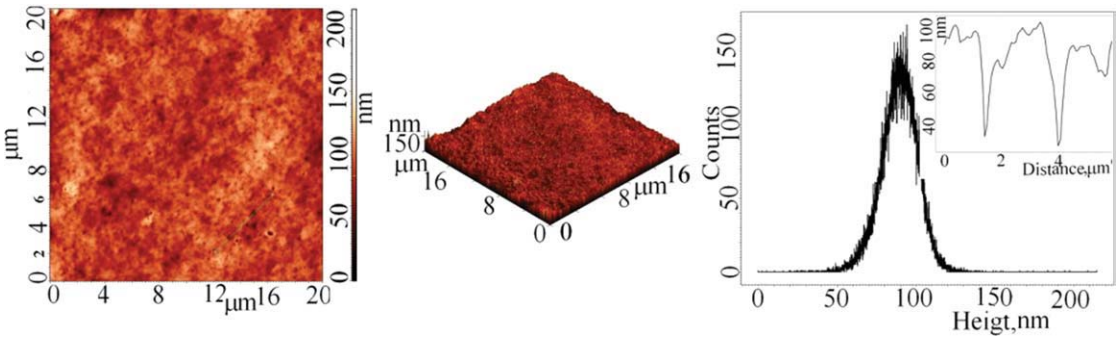

Figure 11 2D and 3D AFM images (scanned area = 20 × 20 μm^2) of PSF–DMOA films obtained from a 60/40 (v/v) DMF/water solution as well as the histogram and surface profile (small plot). [Color figure can be viewed in the online issue, which is available at wileyonlinelibrary.com.]

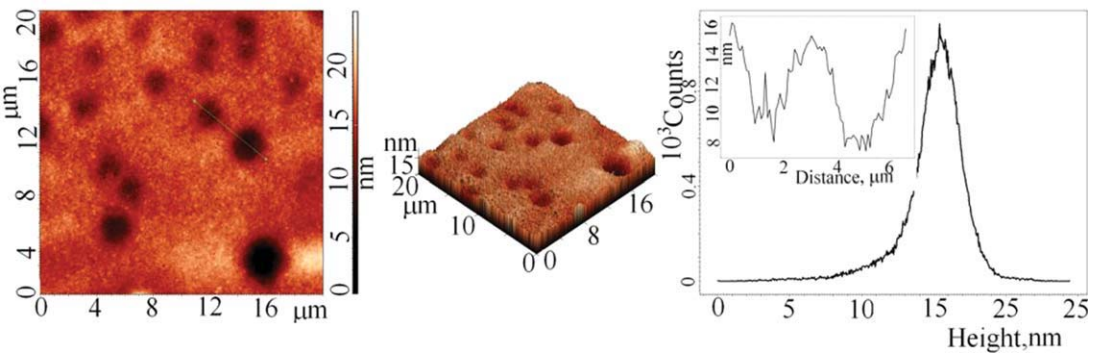

Figure 12 2D and 3D AFM images (scanned area = 20 × 20 μm^2) of PSF–DMOA films obtained from a 50/50 (v/v) DMF/water solution as well as the histogram and surface profile (small plot). [Color figure can be viewed in the online issue, which is available at wileyonlinelibrary.com.]

influenced the AFM images presented in Figures 10–12; a higher water content decreased the thermodynamic quality of the DMF/water solvent mixtures (see Fig. 1). Therefore, for a 60/40 (v/v) DMF/water mixture, the average surface roughness, number of pores, and pore depth were maximum with a minimum area (Table V).

It can be assumed that the specific interactions with the mixed solvents employed in this study modified the PSF–DMOA solubility and determined the modification of the solution properties[29] according to Figure 1.

The plasma treatment effect of the PSF–DMOA films realized in 45/55 (v/v) DMF/MeOH solvent mixtures, illustrated in AFM images (Fig. 13), led to modification of the surface topography, which was reflected by a higher average surface roughness and pore depth and by a decrease in their areas (according

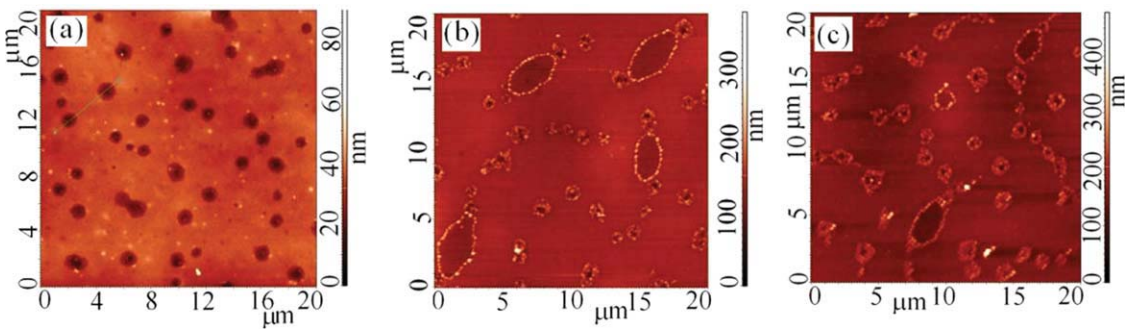

Figure 13 2D AFM images (scanned area = 20 × 20 μm^2) of (a) untreated PSF–DMOA films, (b) plasma-treated PSF–DMOA films immediately after the treatment, and (c) plasma-treated PSF–DMOA films 28 days after the treatment from a 45/55 (v/v) DMF/MeOH solution. [Color figure can be viewed in the online issue, which is available at wileyonlinelibrary.com.]

T6 to Table VI). Figure 13 shows that these modifications, unlike the hydrophobicity reduction (which was reversible after 5 days), remained constant over time.

CONCLUSIONS

The new quaternized PSF prepared by the quaternization of CMPSF with DMOA was investigated to obtain information on its surface tension parameters and surface morphology. The results were correlated with the hydrophilic/hydrophobic properties of the polymers and blood compatibility. The corresponding films were prepared by a dry-cast process in DMF/MeOH and DMF/water mixtures, and the compositions of the solvent/nonsolvent mixtures were selected as a function of polymer solubility. The type of nonsolvent significantly influenced the surface tension parameters, yet the surface hydrophobic characteristics were maintained. Also, a low plasma treatment, besides cleaning the surface, decreased the hydrophobicity; this was a reversible phenomenon.

The AFM images showed that the morphology of the films changed because of the nonsolvents used and the solvent/nonsolvent composition:

- The surface morphology depended on the history of the formed films; this included the thermodynamic quality of the solvents.
- For films prepared from DMF/MeOH solutions, the number of pores and their average size increased according to AFM images, whereas the average surface roughness decreased with the content of the nonsolvent MeOH increasing.
- For films prepared from DMF/water solutions, the presence of water as a nonsolvent in the casting solution decreased the thermodynamic quality of the DMF/water solvent mixtures until a water concentration of 40%, so for the corresponding films, the average surface roughness, the number of pores, and the pore depth were maximum with a minimum area.
- The occurrence of nodules was intensified in organic solvent/organic nonsolvent mixtures, and it was more reduced in organic solvent/water mixtures.
- The interactions and association phenomena of MeOH and water in mixtures with DMF of different compositions affected the surface tension properties and morphology of the PSF–DMOA films.

The studies of quaternized PSF–DMOA showed that the intrinsic viscosity and preferential adsorption were modified, so the solubility depended on the solvent/nonsolvent mixtures. This indicates that

TABLE VI
Pore Characteristics and Surface Roughness Parameters of Plasma-Treated Quaternized PSF Films Prepared from DMF/MeOH Solutions with 20 × 20 μm^2 Scanned Areas Corresponding to 2D AFM Images

	Pore characteristics					Surface roughness		
Solvent mixture (% v/v)	Area (μm^2)	Depth (nm)	Diameter (μm)	Length (μm)	Mean width (μm)	Average roughness (nm)	Root mean square roughness (nm)	Nodule height from height profile (nm)
75/25	—	—	—	—	—	18.84	24.03	130
50/50	0.06	43.19	0.31	0.39	0.16	5.76	9.32	45
45/55	0.07	43.48	0.29	0.48	0.13	9.05	15.76	60

the intrinsic viscosity of a charged polymer solution is an important variable governing the morphology of films and also that chain association in a polymer solution results in macromolecular aggregates and influences the surface topology.

To determine the importance of these modified PSFs, W_s and W_a for red blood cells with respect to PSF–DMOA were investigated. In summary, ΔG_w of the studied polymer and the corresponding values of W_a for blood cells can be used as characterization parameters for predicting cell adhesion onto its surface and hence assessing its compatibility with blood.

References

1. Barikani, M.; Mehdipour-Ataei, S. J Polym Sci Part A: Polym Chem 2000, 38, 1487.
2. Väisänen, P.; Nyström, M. Acta Polytech Scand 1997, 247, 25.
3. Higuchi, A.; Iwata, N.; Tsubaki, M.; Nakagawa, T. J Appl Polym Sci 1988, 36, 1753.
4. Higuchi, A.; Nakagawa, T. J Appl Polym Sci 1990, 41, 1973.
5. Higuchi, A.; Koga, H.; Nakagawa, T. J Appl Polym Sci 1992, 46, 449.
6. Johnson, R. N. In Encyclopedia of Polymer Science and Technology; Herman, F. M.; Norman, G. G.; Bikales, M. N., Eds.; Wiley: New York, 1969; Vol.11, p 447.
7. Vanholder, R. Clin Mater 1992, 10, 87.
8. Lysaght, M. J. Contrib Nephrol 1988, 61, 1.
9. Cases, A.; Reverter, C.; Escolar, G.; Sanz, C.; Lopez-Pedret, J.; Revert, L.; Ordinas, A. Kidney Int 1993, 41, S217.
10. Vanholder, R.; Ringoir, S. Contrib Nephrol 1989, 69, 131.
11. Hopkinson, J. Biotechnology 1985, 3, 225.
12. Tharakan, J. P.; Chau, P. C. Biotech Bioeng 1986, 28, 329.
13. Alsuler, G. L.; Dziewulski, D. M.; Sowek, J. A.; Belfort, G. Biotech Bioeng 1986, 28, 646.
14. Aebischer, P.; Russel, P. C.; Christenson, L.; Panol, G.; Monchik, J. M.; Galletti, P. M. Trans Am Soc Artif Intern Organs 1986, 32, 134.
15. Aebischer, P.; Guenard, V.; Winn, S. R.; Valentini, R. F.; Galletti, P. M. Brain Res 1988, 454, 179.
16. Aebischer, P.; Guenard, V.; Brace, S. J Neurosci 1989, 9, 3590.
17. Guan, R.; Zou, H.; Lu, D.; Gong, C.; Liu, Y. Eur Polym J 2005, 41, 1554.
18. Yu, H.; Huang, Y.; Ying, H.; Xiao, C. Carbohydr Polym 2007, 69, 29.
19. Ioan, S.; Filimon, A.; Avram, E. J Appl Polym Sci 2006, 101, 524.
20. Filimon, A.; Avram, E.; Ioan, S. J Macromol Sci Phys 2007, 46, 3.
21. Idris, A.; Zain, N. M. J Teknol 2006, 44, 27.
22. Kochkodan, V.; Tsarenko, S.; Potapchenko, N.; Kosinova, V.; Goncharuk, V. Desalination 2008, 220, 380.
23. Guiver, M. D.; Black, P.; Tam, C. M.; Deslandes, Y. J Appl Polym Sci 1993, 48, 1597.
24. Avram, E.; Butuc, E.; Luca, C. J Macromol Sci Pure Appl Chem 1997, 34, 1701.
25. Avram, E. Polym-Plast Technol Eng 2001, 40, 275.
26. Luca, C.; Avram, E.; Petrariu, I. J Macromol Sci Chem 1988, 25, 345.
27. Ghimici, L.; Avram, E. J Appl Polym Sci 2003, 90, 465.
28. Ioan, S.; Filimon, A.; Avram, E. Polym Eng Sci 2006, 46, 827.
29. Ioan, S.; Filimon, A.; Avram, E. J Macromol Sci Phys 2005, 44, 129.
30. Ioan, S.; Filimon, A.; Avram, E.; Ioanid, G. e-Polymers 2007, 031, 1.
31. Filimon, A.; Albu, R. M.; Avram, E.; Ioan, S. J Macromol Sci 2010, 49, 207.
32. Filimon, A.; Avram, E.; Dunca, S.; Stoica, I.; Ioan, S. J Appl Polym Sci 2009, 112, 1808.
33. Ström, G.; Fredriksson, M.; Stenius, P. J Colloid Interface Sci 1987, 119, 352.
34. van Oss, C. J.; Ju, L.; Chaudhury, M. K.; Good, R. J. J Colloid Interface Sci 1989, 128, 313.
35. Yildirim, E. H. In Handbook of Surface and Colloid Chemistry; Birdi, K. S., Ed.; CRC: Boca Raton, FL, 1997; Chapter 9, p 265.
36. Gonzalez-Martin, M. L.; Janczuk, B.; Labajos-Broncano, L.; Bruque, J. M. Langmuir 1997, 13, 5991.
37. Busscher, H. J.; van Pelt, A. W. J.; de Boer, P.; de Jong, H. P.; Arends, J. Colloids Surf 1984, 9, 319.
38. Vijayanand, K.; Deepak, K.; Pattanayak, D. K.; Rama Mohan, T. R.; Banerjee, R. Trends Biomater Artif Organs 2005, 18, 73.
39. Owens, D. K.; Wendt, R. C. J Appl Polym Sci 1969, 13, 1741.
40. Rabel, W. Phys Blätter 1977, 33, 151.
41. Kälble, D. H. J Adhes 1969, 1, 102.
42. van Os, C. J.; Good, R. J.; Chaudhury, M. K. Langmuir 1988, 4, 884.
43. van Oss, C. J.; Ju, L.; Chaudhury, M. K.; Good, R. J. Chem Rev 1988, 88, 927.
44. van Oss, C. J. Interfacial Forces in Aqueous Media; Marcel Dekker: New York, 1994.
45. Rankl, M.; Laib, R.; Seeger, S. Colloids Surf B 2003, 30, 177.
46. Good, R. J.; van Oss, C. J. Wettability; Plenum: New York, 1992.
47. Wu, W.; Giese, R. F., Jr.; van Oss, C. J. Langmuir 1995, 11, 379.
48. Della Volpe, C.; Maniglio, D.; Brugnara, M.; Siboni, S.; Morra, M. J Colloid Interface Sci 2004, 271, 434.
49. Kwok, D. Y.; Ng, H.; Neumann, A. W. J Colloid Interface Sci 2000, 225, 323.
50. Qian, J. W.; An, Q. F.; Wang, L. N.; Zhang, L.; Shen, L. J Appl Polym Sci 2005, 97, 1891.
51. Huang, D. H.; Ying, Y. M.; Zhuang, G. Q. Macromolecules 2000, 33, 461.
52. Hopkins, A. R.; Rasmussen, P. G.; Basheer, R. A. Macromolecules 1996, 297, 838.
53. Bryjak, M.; Pozniak, G.; Gancarz, I.; Tylus, W. Desalination 2004, 163, 231.
54. Gancarz, I.; Pozniak, G.; Bryjak, M. Eur Polym J 1999, 35, 1419.
55. Faibish, R. S.; Yoshida, W.; Cohen, Y. J Colloid Interface Sci 2002, 256, 341.
56. Dourado, F.; Gama, F. M.; Chibowski, E.; Mota, M. J Adhes Sci Technol 1998, 12, 1081.
57. van Oss, C. J.; Giese, R. F. Clays Clay Miner 1995, 43, 474.